



Guiding and confining of light in a two-dimensional synthetic space using electric fields

HAMIDREZA CHALABI,^{1,2,5} SABYASACHI BARIK,^{1,2,3}  SUNIL MITTAL,^{1,2} THOMAS E. MURPHY,^{1,3} 
MOHAMMAD HAFEZI,^{1,2,3} AND EDO WAKS^{1,2,3,4}

¹Department of Electrical and Computer Engineering and Institute for Research in Electronics and Applied Physics, University of Maryland, College Park, Maryland 20742, USA

²Joint Quantum Institute, University of Maryland, College Park, Maryland 20742, USA

³Department of Physics, University of Maryland, College Park, Maryland 20742, USA

⁴e-mail: edowaks@umd.edu

⁵e-mail: hchalabi@umd.edu

Received 18 December 2019; revised 8 April 2020; accepted 16 April 2020 (Doc. ID 386347); published 12 May 2020

Synthetic dimensions provide a promising platform for photonic quantum simulations. Manipulating the flow of photons in these dimensions requires an electric field. However, photons do not have charge and do not directly interact with electric fields. Therefore, alternative approaches are needed to realize electric fields in photonics. One approach is to use engineered gauge fields that can mimic the effect of electric fields and produce the same dynamical behavior. Here, we demonstrate such an electric field for photons propagating in a two-dimensional synthetic space. Generation of electric fields in a two-dimensional synthetic lattice provides the possibility to guide photons and to trap them through the creation of quantum confined structures. We achieve this using a linearly time-varying gauge field generated by direction-dependent phase modulations. We show that the generated electric field leads to Bloch oscillations and the revival of the state after a certain number of steps dependent on the field strength. We measure the probability of the revival and demonstrate a good agreement between the observed values and the theoretically predicted results. Furthermore, by applying a nonuniform electric field, we show the possibility of waveguiding photons. Ultimately, our results open up new opportunities for manipulating the propagation of photons with potential applications in photonic quantum simulations. © 2020 Optical Society of America under the terms of the OSA Open Access Publishing Agreement

<https://doi.org/10.1364/OPTICA.386347>

1. INTRODUCTION

Photons are promising candidates for implementing quantum simulations due to their wave characteristics that exhibit strong interference effects. Recently, numerous complicated quantum simulations have been performed using photonic systems by molding the flow of light in real space [1–4]. However, there are limitations for these systems to simulate the higher-dimensional quantum systems needed for modeling a wider class of Hamiltonians. Synthetic dimensions provide a promising alternative approach for photonic quantum simulations in a scalable and resource-efficient way without requiring complex photonic circuits [5–18]. One powerful technique to implement a synthetic space is through time multiplexing [19–24], which can scale to a higher number of dimensions efficiently. But significant challenges remain to fully control the evolution of photons in synthetic spaces.

One important challenge is that photons do not directly interact with electromagnetic fields because of their lack of charge. This limitation makes it difficult for photons to simulate the complex dynamical behavior of electrons or atoms. But significant progress in the past decade has led to the development of techniques to

engineer magnetic and electric fields for photons [25–28]. In particular, the realization of synthetic magnetic fields has led to the exploration of topological physics in photonic systems [29] and the measurement of associated topological invariants [18,30–32]. Similarly, various ways to engineer electric fields have been reported in real dimensional photonic circuits [33–35]. One outcome of applying a constant electric field in periodic systems is the generation of state revivals known as Bloch oscillations, originally predicted in electronic systems [36–38]. Bloch oscillations have been observed in photonic systems such as coupled optical waveguide arrays [39–45] and one-dimensional quantum walks of photons [46,47]. Bloch oscillations in one dimension have also been explored using frequency as a synthetic dimension [48–50]. However, the extension of electric fields to two-dimensional synthetic spaces and demonstration of the associated Bloch oscillations has not yet been explored. Furthermore, the introduction of nonuniform electric fields in two-dimensional quantum walks remains largely unexplored. Such nonuniform fields could open up new methods to achieve quantum confinement for trapping and guiding of quantum walkers in synthetic dimensions.

Here we demonstrate an electric field for photons in a two-dimensional synthetic space. We use time multiplexing as a versatile platform to create the synthetic space and a time-varying gauge field to create the electric field. Under the application of a constant electric field, we show that photons return to the original state after a certain number of steps and thus demonstrate Bloch oscillations. Furthermore, by generating a spatially nonuniform electric field, we realize a synthetic quantum well, which guides photons without the use of a bandgap. Instead, the guiding is mediated by a discontinuous gauge field. This guiding effect does not have a direct analogue in one-dimensional systems, and it is therefore unique to two-dimensional systems with nonuniform fields.

2. RESULTS AND DISCUSSION

In our time-multiplexed photonic quantum walk, the quantum walker state space is mapped into time delays of optical pulses. The experimental setup is a closed-loop fiber architecture composed of two beam splitters with their ports connected to fibers of different lengths mapping the $\pm x$ and $\pm y$ directions to different time delays. Full details of the experimental setup are explained in Supplement 1. One complete propagation of an optical pulse around the loop is equivalent to the hopping of the walker to one of the four possible corners in the synthetic space (Fig. 1). In the first part of each time step, the quantum walker moves toward the right or left directions and acquires opposite phase shifts. In the second part of the time step, the quantum walker chooses to move toward the up or down direction. Semiconductor optical amplifiers as well as polarization controllers are used in the setup to compensate for the losses and polarization changes that the optical pulses experience in each round-trip, respectively. The quantum walk distribution at each time step is studied via two photodetectors analyzing two channels that we refer to as the up and down channels (see Fig. S1 of Supplement 1). A single incident laser pulse that is injected into the up channel initializes the quantum walk evolution from the origin in the synthetic space.

In this setup, we use electro-optic modulators that can introduce desired phase shifts to pulses moving to the right or left directions to generate the synthetic gauge field. Specifically, here we implement a linearly time-varying gauge field ($\vec{A} = -\mathcal{E}t\hat{x}$, in which t denotes the time step and \hat{x} is the unit vector in the x direction) that leads to the generation of a constant electric field

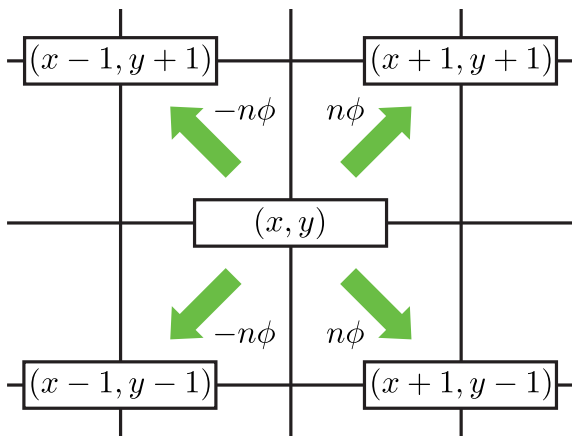


Fig. 1. Applied phase modulation scheme for the n th step of the quantum walk.

($\vec{\mathcal{E}} = -\partial\vec{A}/\partial t$). To implement this gauge field, a phase modulation needs to be applied that varies with the time step. Figure 1 depicts the synthetic lattice with the required phase modulation criteria describing the amount of phase that the walker accumulates in hopping to the four possible corners at time step n .

This method of generating an electric field is distinguished from the approaches based on position-dependent but time-independent gauge fields [51–53] used in discrete-time quantum walks. In these approaches, an effective linear electric potential $V = -\mathcal{E}x$ is implemented, which leads to the generation of electric fields based on $\vec{\mathcal{E}} = -\nabla V$. In order to create such a gauge field in discrete-time quantum walks, the unitary operation in each time step must have an extra term relative to the standard quantum walk evolution operator U_0 as $U_\phi = e^{i\phi x} U_0$. In contrast, the current approach does not require any coordinate-dependent unitary operation to generate an electric field. This is of particular interest for time-multiplexed quantum walks, as it relaxes the need for any variation of phase modulations during each time step. The equivalence of these approaches can be understood in terms of a gauge transformation [54]. The similarity between the approach used and the conventional coordinate-based method of implementing an electric field in a two-dimensional quantum walk [53] is described in Supplement 1. We show that the total phase accumulated in some sample closed loops that start from the origin and return to it in both pictures are the same. In fact, this similarity holds for any closed path starting from the origin and ending at it.

The application of the electric field in our two-dimensional discrete-time quantum walk will lead to Bloch oscillations and the revival of the quantum state. This can be intuitively explained through the band diagram structure of the system. In the band structure, we refer to energy eigenvalues of the system as pseudo-energies due to the time dependency of the gauge fields to distinguish them from the term quasi-energies we used for the case of time-independent gauge fields. Due to the periodicity of the system by time, pseudo-energy values are between $-\pi$ and π similar to quasi-energies. As we show in Supplement 1, for a phase modulation with a fractional value of ϕ as $\phi = 2\pi/q$, the band structure has $2q$ bands. The analytical expressions for the pseudo-energy band structure under such a phase modulation are given by

$$E_{n,\pm,k_x,k_y} = \frac{2n\pi}{q} \pm \frac{1}{q} \arccos \left(\cos \left(\frac{\pi q}{2} \right) (\sin^q k_y - 1) - \cos \left(qk_x + \frac{\pi q}{2} \right) \sin^q k_y \right), \quad (1)$$

where k_x and k_y are the momentum wave vectors in inverse synthetic space and $n \in \mathbb{Z}$. This expression for $q = 1$ returns to the form of $E_\pm = \pm \arccos(\sin(k_x) \sin(k_y))$, which represents the band structure for the quantum walk under no effective applied gauge field [55]. Figure 2 shows the band diagrams for three different values of the phase modulations. As this figure shows, in these band diagrams there exists no bandgap. By increasing q , the bands become flatter and equidistant from each other, and the corresponding group velocities tend toward zero. As has been demonstrated in one-dimensional quantum walks, this will lead to the revival of the quantum walk with high probability [52]. This band flattening also occurs in the two-dimensional Floquet quantum walks considered here, which will lead to the return of the quantum walker toward the origin after q steps. In our system,

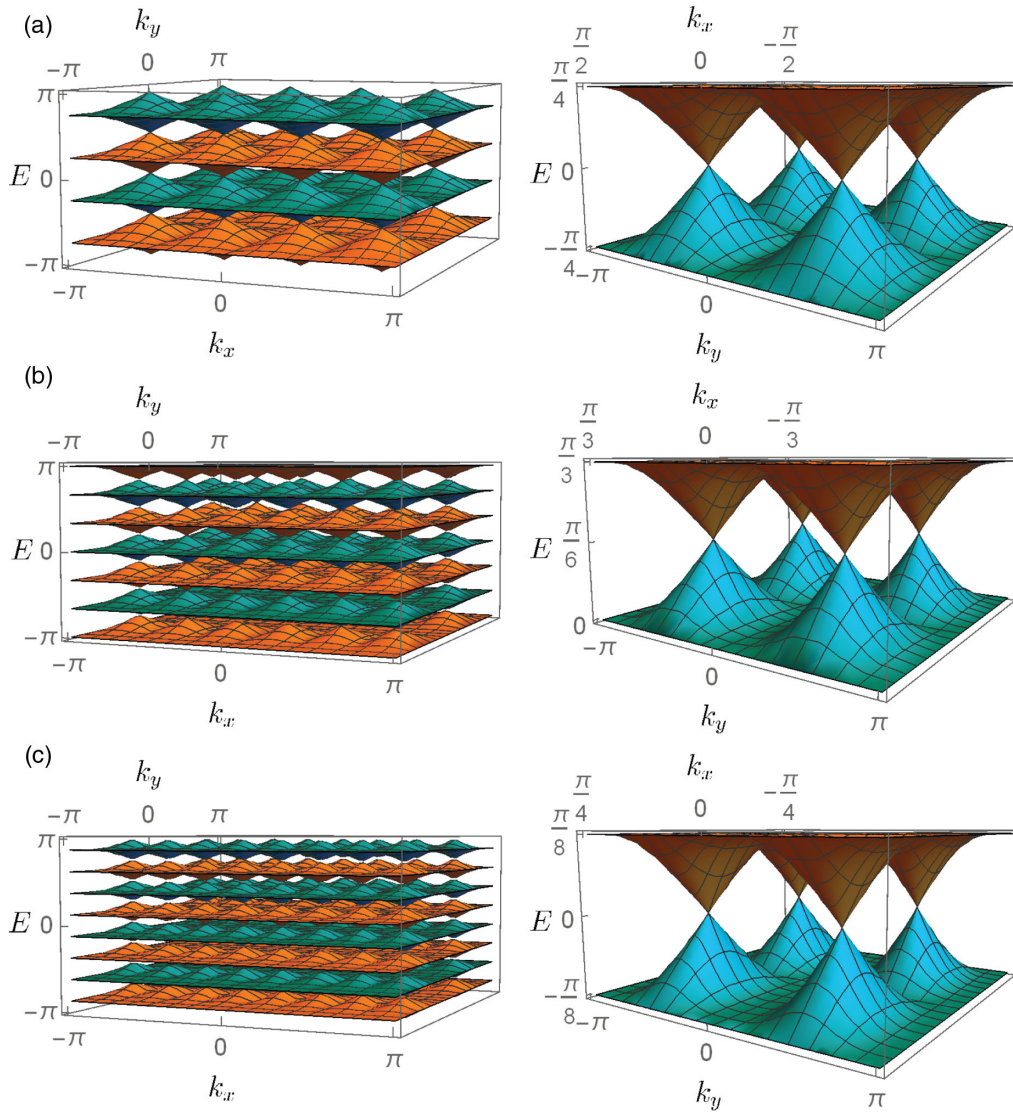


Fig. 2. Pseudo energy band diagrams of the two-dimensional quantum walk for different gauge field strengths: (a) $\phi = \pi/2$, (b) $\phi = \pi/3$, and (c) $\phi = \pi/4$. In each row the left figure shows the full band diagram, while the right one shows the zoomed in part of the band diagram.

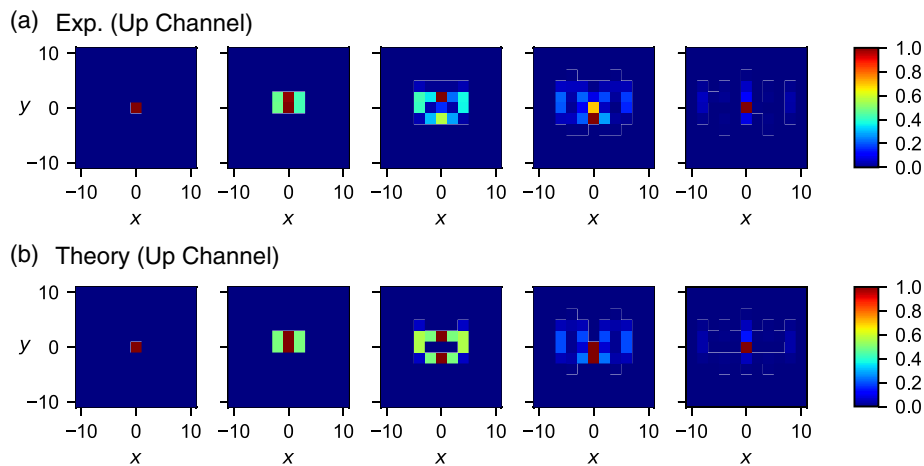


Fig. 3. (a) Experimental observations and (b) theoretical predictions of the evolution of the quantum walk distribution under the application of the time-dependent phase modulation with $\phi = \pi/4$. The columns from left to right show the distributions at time steps of 0, 2, 4, 6, and 8, respectively. In these plots, all the distributions are normalized to their maximum.

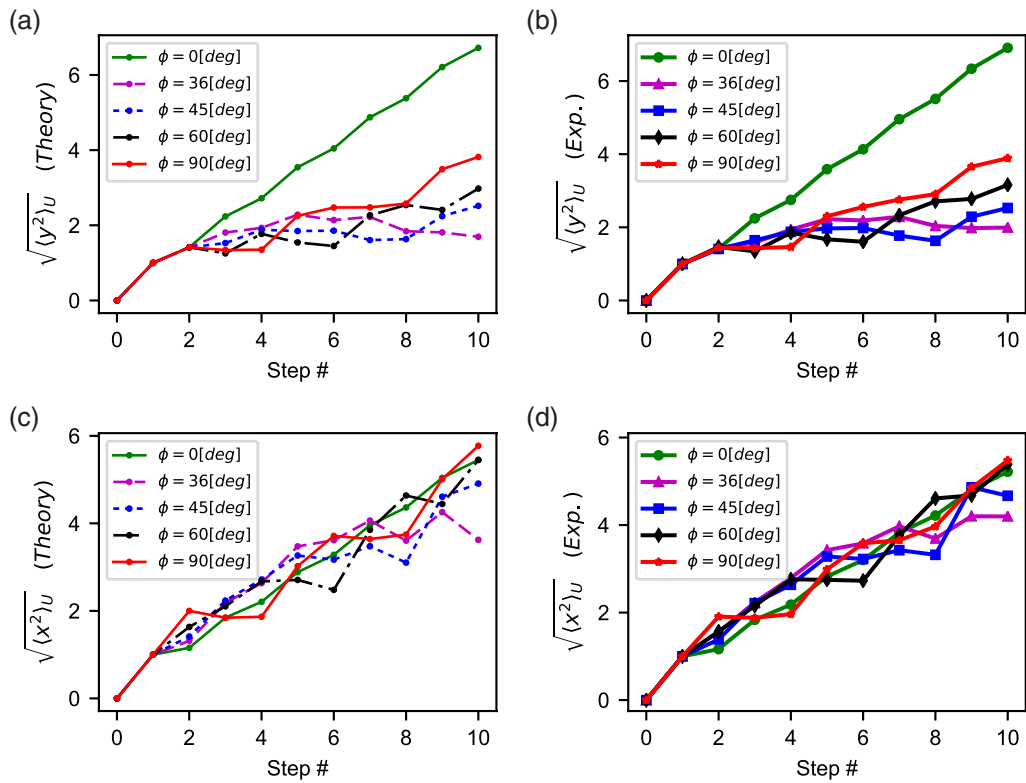


Fig. 4. Theoretical values for the quadratic means of (a) y and (c) x as a function of the time step for different gauge field strengths. Experimental values for the quadratic means of (b) y and (d) x as a function of the time step for different gauge field strengths.

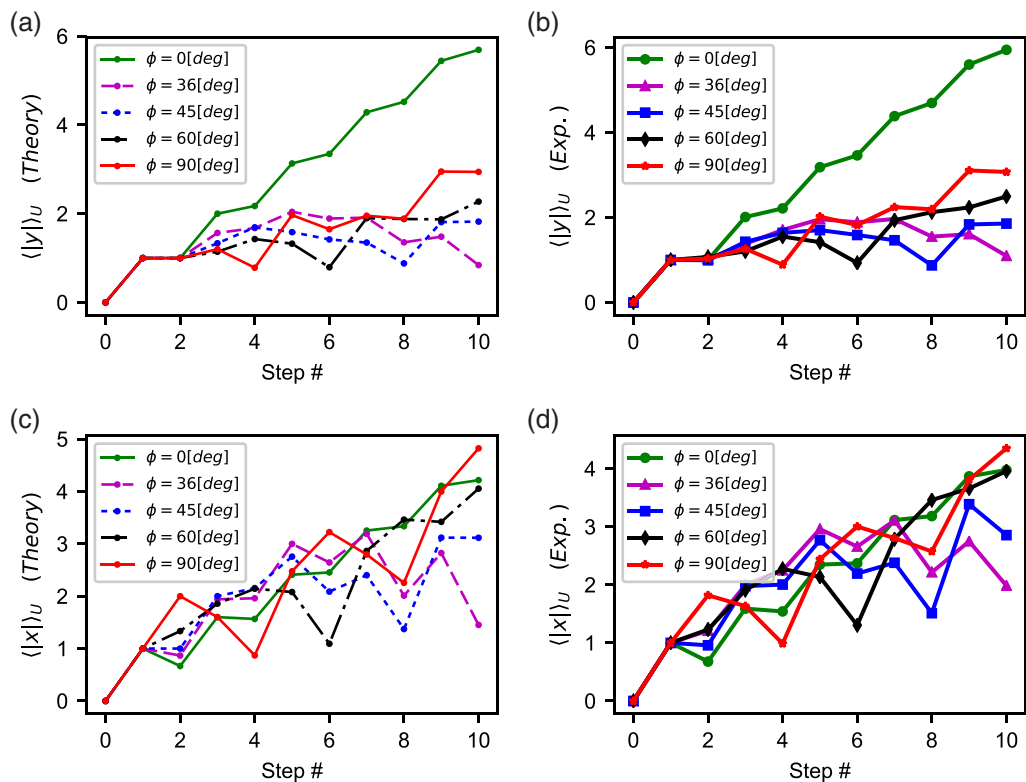


Fig. 5. Theoretical values for the norm ones of (a) y and (c) x as a function of the time step for different gauge field strengths. Experimental values for the norm ones of (b) y and (d) x as a function of the time step for different gauge field strengths.

the application of an electric field in the x direction will lead to the revival of the quantum walk not only in the x direction but also in the y direction (see Supplement 1). This is quite interesting that the revival happens not only in the direction of the applied electric field but also in the orthogonal direction.

To experimentally demonstrate Bloch oscillations in our 2D time-multiplexed quantum walk caused by the applied electric field, we investigate the evolution of the quantum walk distribution at different time steps. In order to measure the quantum walk distribution, we measure the power of the optical pulses received by the photodetectors at different time delays for each time step. Figure 3(a) shows the experimentally measured quantum walk distributions at different time steps. This figure demonstrates state revival under the application of the time-varying gauge field due to the uniform electric field generated. The phase strength of the applied electric field in this case is $\phi = \pi/4$. As this figure shows, after eight steps, the quantum walker returns to the origin with a probability as high as 0.6. The experimental results are in good agreement with the corresponding theoretical predictions shown in Fig. 3(b).

We measure the quantum walk distribution at different time steps under the application of the proposed time-varying gauge fields with different phases ($\phi = 0$ [deg], $\phi = 90$ [deg],

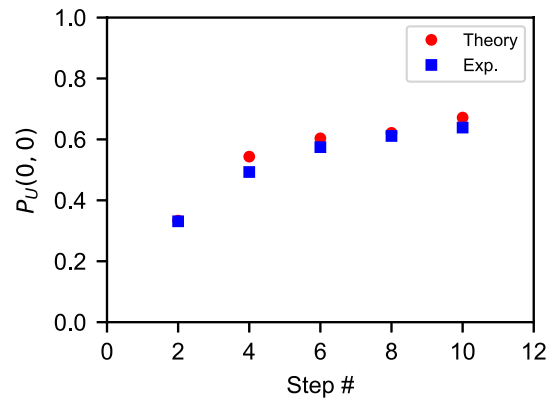


Fig. 6. Probability of revival: experimental (blue solid squares) and theoretical (red solid circles) probabilities of the walker returning to the origin with respect to the required number of steps for the revival to happen. The error bars in the measurements are smaller than the size of the plotted data points.

$\phi = 60$ [deg], $\phi = 45$ [deg], and $\phi = 36$ [deg]). Using the measured probability distributions, we can calculate the statistical averages of the distribution at different time steps. Specifically, we calculate the quadratic means as well as the norm ones of the x and

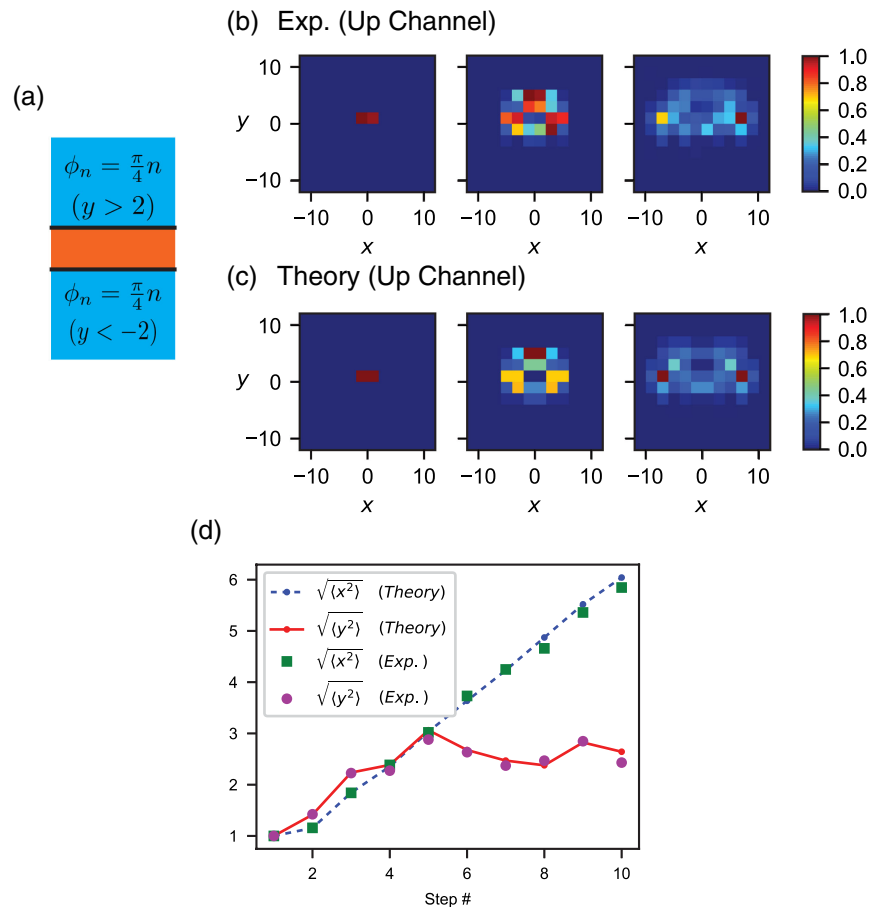


Fig. 7. Confinement of the quantum walker through the application of a discontinuous electric field. (a) Schematic describing the phase modulation pattern in the synthetic space that leads to a zero electric field for $-2 < y < 2$ and a nonzero electric field outside this range. (b) Experimental observations and (c) theoretical predictions of the evolution of the quantum walk distribution under the discontinuous electric field. The columns from left to right show the distributions at time steps of 1, 5, and 9, respectively. All the distributions are normalized to their maximum. (d) Experimentally measured and theoretically predicted quadratic means of x and y as a function of the time step. The error bars in the measurements are smaller than the size of the plotted data points.

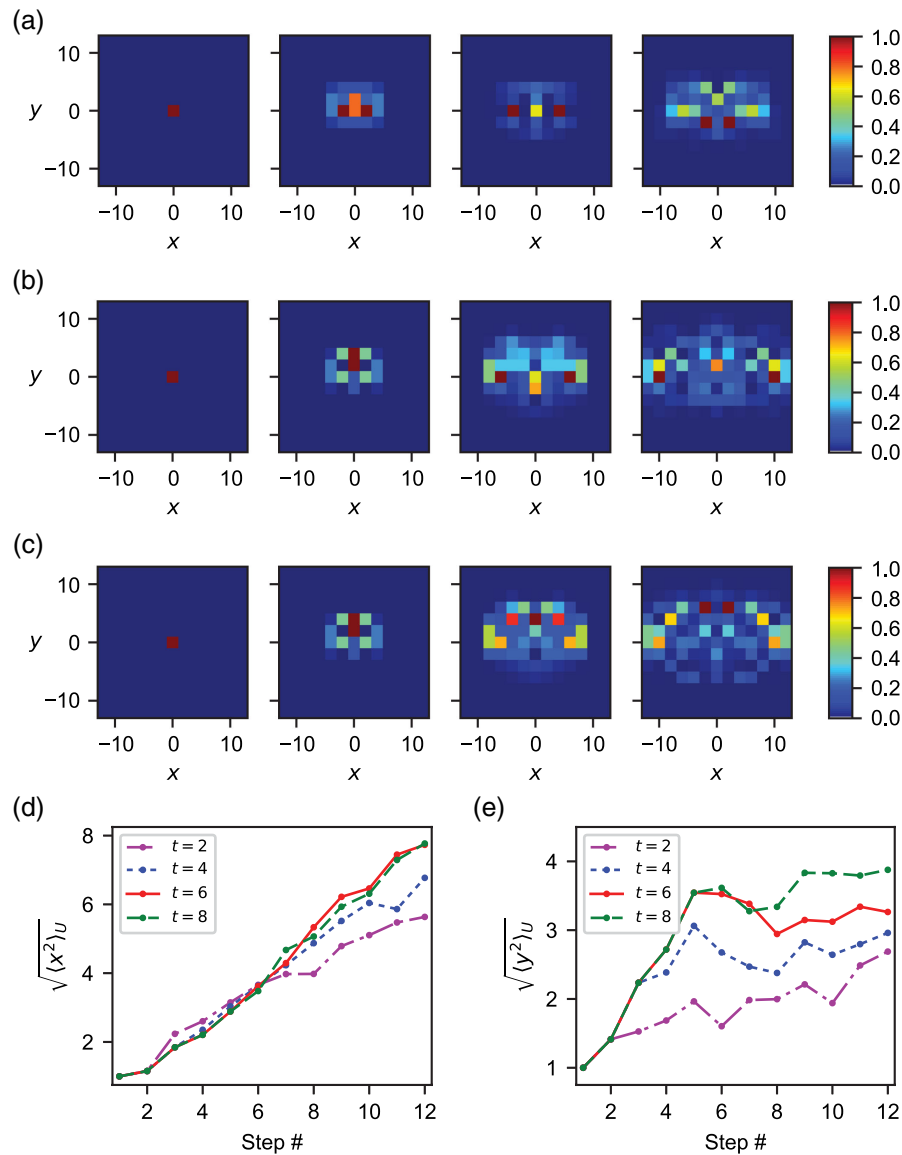


Fig. 8. Theoretical predictions of the evolution of the quantum walk distribution under the discontinuous electric field for the thickness of (a) $t = 2$, (b) $t = 6$, and (c) $t = 8$. The columns from left to right show the distributions at time steps of 0, 4, 8, and 12, respectively. All the distributions are normalized to their maximum. Quadratic means of (d) x and (e) y as a function of the time step for different thicknesses of the discontinuity.

y coordinates at different time steps. The corresponding results are shown in Figs. 4 and 5. As these results show, the quadratic means as well as the norm ones of x and y tend toward the local minimum values after $2\pi/\phi$ steps. The variational behaviors of these quantities with the time step confirm the revival effect in both the x and y directions and are in good agreement with the theoretically predicted results.

To quantify the effect of the gauge field on the revival of the quantum state, we measure the probability of the walker returning to the origin [revival probability $P_U(0, 0)$] as a function of the number of steps taken (Fig. 6). We measure this probability for different time-varying phase modulations after the appropriate number of time steps ($2\pi/\phi$ steps) needed for the revival to happen. As shown in Fig. 6, the revival probability increases with increasing number of steps. Additionally, this figure indicates that the experimental results are in good agreement with the theoretical predictions. In Supplement 1], we demonstrate that by decreasing

the phase modulation ϕ , the revival probability increases and tends toward unity.

We are not restricted to implementing only uniform electric fields in our two-dimensional quantum walk. Spatially discontinuous electric fields can also be created by simply controlling the modulation pattern of the phase modulators. This provides the possibility to perform waveguiding in the synthetic space using gauge fields. Figure 7(a) shows an example of a discontinuous electric field in a two-dimensional synthetic space. In this configuration, the electric field is zero in the $-2 < y < 2$ region and nonzero outside this range. Due to the boundary created by the discontinuous gauge fields, the quantum random walk evolution is mainly confined to the region where the electric field is equal to zero. Figure 7(b) presents the experimentally measured quantum walk distributions at different time steps showing the trapping caused by the existence of the boundaries in the electric field pattern. The experimentally measured results are in good agreement

with the theoretical predictions shown in Fig. 7(c). Additionally, more quantitative agreement can be inferred based on Fig. 7(d) depicting the variations of the quadratic means as functions of the time step. This figure clearly shows that the presence of boundaries in the field pattern has led to the confinement of the quantum walk in the y ribbon. We note that this confinement is not induced by a bandgap and is therefore physically distinct from the confinement in conventional crystal heterostructures.

We can also investigate the evolution of the quantum walk for other thicknesses of the region with the electric field equal to zero. The evolution of the quantum walk for different thicknesses of the y ribbon are shown in Figs. 8(a)–8(c). These results correspond to the thicknesses of $t = 2$, $t = 6$, and $t = 8$, respectively. The obtained results show that the confinement in the y direction holds for other thicknesses as well. In Figs. 8(d) and 8(e), we have shown the variations of the quadratic means of x and y for various thicknesses as functions of the time step. As these figures show, the confinement in the y direction holds for all the considered thicknesses. However, it takes increasing number of time steps for higher thicknesses to see the effect of confinement due to the finite speed of the quantum walkers to reach the discontinuity. None of the three regions shown in Fig. 7(a) supports a bandgap, which thus demonstrates that the confinement is directly induced by the gauge field itself. These results demonstrate the possibility of using a nonuniform electric field in order to guide the path of the quantum walk in a desired fashion. This is in a sense similar to the guiding of light in a waveguide. Here, however, the required refractive index contrast between the core and the cladding of a waveguide is emulated using discontinuous synthetic electric fields.

3. CONCLUSION

In this work, we studied the time evolution of a quantum random walk under a time-varying gauge field in a two-dimensional synthetic space. Using a linearly time-varying phase modulation, an electric field acting on photonic quantum walkers can be created. Creation of an electric field in two-dimensional discrete time quantum walks with the possibility of controlling its spatial variation enables the implementation of quantum confined structures with potential applications in trapping and guiding of quantum walkers. Our findings demonstrate that, under the influence of a uniform electric field, a complete revival caused by Bloch oscillations happens in two-dimensional quantum walks. This revival becomes more accurate as we increase the number of steps. Moreover, by exploiting spatially varying electric fields, we demonstrated and analyzed a new type of quantum confined structure: a synthetic quantum well. This structure, which has no analogue in one-dimensional systems, guides quantum walkers when there is no bandgap. The use of spatially varying electric fields in synthetic dimensions opens up the possibility to explore a broad range of quantum confined structures in discrete time quantum walks using smoothly varying fields as well as confinement in higher-dimensional systems. Time-multiplexed synthetic space provides a particularly compelling implementation, because it can realize quantum walks in higher-dimensional lattices unlike spatial quantum walks, which are limited to three dimensions.

While we demonstrated the Bloch oscillation for a quantum walk initiated with classical coherent laser pulses, the same physics holds at the single-photon level. The obtained results can be extended to the investigation of the effect of dynamic localization [56–62]. Our demonstration of an electric field for photons

in time-multiplexed synthetic lattices could also have potential applications in photonic quantum simulations, for example, multiphoton interference and Boson sampling in the time domain [63], and the realization of photonic lattices with strong nonlinearities mediated via artificial atoms like quantum dots [64,65]. Our results ultimately greatly expand the types of Hamiltonians that could be realized for applications in photonic quantum simulation and computation.

Funding. Air Force Office of Scientific Research (FA9550-16-1-0323); National Science Foundation (PHYS. 1415458, PHY-1430094); Center for Distributed Quantum Information.

Disclosures. The authors declare no conflicts of interest.

See [Supplement 1](#) for supporting content.

REFERENCES AND NOTE

1. C. Sparrow, E. Martín-López, N. Maraviglia, A. Neville, C. Harrold, J. Carolan, Y. N. Joglekar, T. Hashimoto, N. Matsuda, J. L. O'Brien, D. P. Tew, and A. Laing, "Simulating the vibrational quantum dynamics of molecules using photonics," *Nature* **557**, 660–667 (2018).
2. X.-S. Ma, B. Dakic, W. Naylor, A. Zeilinger, and P. Walther, "Quantum simulation of the wavefunction to probe frustrated Heisenberg spin systems," *Nat. Phys.* **7**, 399–405 (2011).
3. B. P. Lanyon, J. D. Whitfield, G. G. Gillett, M. E. Goggin, M. P. Almeida, I. Kassal, J. D. Biamonte, M. Mohseni, B. J. Powell, M. Barbieri, A. Aspuru-Guzik, and A. G. White, "Towards quantum chemistry on a quantum computer," *Nat. Chem.* **2**, 106–111 (2010).
4. A. Aspuru-Guzik and P. Walther, "Photonic quantum simulators," *Nat. Phys.* **8**, 285–291 (2012).
5. C. Navarrete-Benlloch, A. Pérez, and E. Roldán, "Nonlinear optical Galton board," *Phys. Rev. A* **75**, 062333 (2007).
6. D. Bouwmeester, I. Marzoli, G. P. Karman, W. Schleich, and J. P. Woerdman, "Optical Galton board," *Phys. Rev. A* **61**, 013410 (1999).
7. B. A. Bell, K. Wang, A. S. Solntsev, D. N. Neshev, A. A. Sukhorukov, and B. J. Eggleton, "Spectral photonic lattices with complex long-range coupling," *Optica* **4**, 1433–1436 (2017).
8. C. Qin, F. Zhou, Y. Peng, D. Sounas, X. Zhu, B. Wang, J. Dong, X. Zhang, A. Alù, and P. Lu, "Spectrum control through discrete frequency diffraction in the presence of photonic gauge potentials," *Phys. Rev. Lett.* **120**, 133901 (2018).
9. A. Dutt, M. Minkov, Q. Lin, L. Yuan, D. A. B. Miller, and S. Fan, "Experimental band structure spectroscopy along a synthetic dimension," *Nat. Commun.* **10**, 3122 (2019).
10. A. Regensburger, C. Bersch, M.-A. Miri, G. Onishchukov, D. N. Christodoulides, and U. Peschel, "Parity–time synthetic photonic lattices," *Nature* **488**, 167–171 (2012).
11. E. Lustig, S. Weimann, Y. Plotnik, Y. Lumer, M. A. Bandres, A. Szameit, and M. Segev, "Photonic topological insulator in synthetic dimensions," *Nature* **567**, 356–360 (2019).
12. Q. Lin, M. Xiao, L. Yuan, and S. Fan, "Photonic Weyl point in a two-dimensional resonator lattice with a synthetic frequency dimension," *Nat. Commun.* **7**, 13731 (2016).
13. Q. Lin, X.-Q. Sun, M. Xiao, S.-C. Zhang, and S. Fan, "A three-dimensional photonic topological insulator using a two-dimensional ring resonator lattice with a synthetic frequency dimension," *Sci. Adv.* **4**, eaat2774 (2018).
14. L. Yuan, M. Xiao, Q. Lin, and S. Fan, "Synthetic space with arbitrary dimensions in a few rings undergoing dynamic modulation," *Phys. Rev. B* **97**, 104105 (2018).
15. S. K. Goyal, F. S. Roux, A. Forbes, and T. Konrad, "Implementing quantum walks using orbital angular momentum of classical light," *Phys. Rev. Lett.* **110**, 263602 (2013).
16. F. Cardano, F. Massa, H. Qassim, E. Karimi, S. Slussarenko, D. Paparo, C. de Lisio, F. Sciarrino, E. Santamato, R. W. Boyd, and L. Marrucci, "Quantum walks and wavepacket dynamics on a lattice with twisted photons," *Sci. Adv.* **1**, e1500087 (2015).
17. F. Cardano, M. Maffei, F. Massa, B. Piccirillo, C. de Lisio, G. De Filippis, V. Cataudella, E. Santamato, and L. Marrucci, "Statistical moments of

- quantum-walk dynamics reveal topological quantum transitions," *Nat. Commun.* **7**, 11439 (2016).
18. F. Cardano, A. D'Errico, A. Dauphin, M. Maffei, B. Piccirillo, C. de Lisio, G. De Filippis, V. Cataudella, E. Santamato, L. Marrucci, M. Lewenstein, and P. Massignan, "Detection of Zak phases and topological invariants in a chiral quantum walk of twisted photons," *Nat. Commun.* **8**, 15516 (2017).
 19. A. Schreiber, K. N. Cassemiro, V. Potoček, A. Gábris, P. J. Mosley, E. Andersson, I. Jex, and C. Silberhorn, "Photons walking the line: a quantum walk with adjustable coin operations," *Phys. Rev. Lett.* **104**, 050502 (2010).
 20. A. Schreiber, K. N. Cassemiro, V. Potoček, A. Gábris, I. Jex, and C. Silberhorn, "Decoherence and disorder in quantum walks: from ballistic spread to localization," *Phys. Rev. Lett.* **106**, 180403 (2011).
 21. A. Schreiber, A. Gábris, P. P. Rohde, K. Laiho, M. Stefanak, V. Potoček, C. Hamilton, I. Jex, and C. Silberhorn, "A 2D quantum walk simulation of two-particle dynamics," *Science* **336**, 55–58 (2012).
 22. T. Nitsche, F. Elster, J. Novotný, A. Gábris, I. Jex, S. Barkhofen, and C. Silberhorn, "Quantum walks with dynamical control: graph engineering, initial state preparation and state transfer," *New J. Phys.* **18**, 063017 (2016).
 23. S. Barkhofen, T. Nitsche, F. Elster, L. Lorz, A. Gábris, I. Jex, and C. Silberhorn, "Measuring topological invariants in disordered discrete-time quantum walks," *Phys. Rev. A* **96**, 033846 (2017).
 24. C. Chen, X. Ding, J. Qin, Y. He, Y.-H. Luo, M.-C. Chen, C. Liu, X.-L. Wang, W.-J. Zhang, H. Li, L.-X. You, Z. Wang, D.-W. Wang, B. C. Sanders, C.-Y. Lu, and J.-W. Pan, "Observation of topologically protected edge states in a photonic two-dimensional quantum walk," *Phys. Rev. Lett.* **121**, 100502 (2018).
 25. M. Hafezi, E. A. Demler, M. D. Lukin, and J. M. Taylor, "Robust optical delay lines with topological protection," *Nat. Phys.* **7**, 907–912 (2011).
 26. S. Mittal, J. Fan, S. Faez, A. Migdall, J. M. Taylor, and M. Hafezi, "Topologically robust transport of photons in a synthetic gauge field," *Phys. Rev. Lett.* **113**, 087403 (2014).
 27. M. C. Rechtsman, J. M. Zeuner, Y. Plotnik, Y. Lumer, D. Podolsky, F. Dreisow, S. Nolte, M. Segev, and A. Szameit, "Photonic Floquet topological insulators," *Nature* **496**, 196–200 (2013).
 28. K. Fang, Z. Yu, and S. Fan, "Realizing effective magnetic field for photons by controlling the phase of dynamic modulation," *Nat. Photonics* **6**, 782–787 (2012).
 29. T. Ozawa, H. M. Price, A. Amo, N. Goldman, M. Hafezi, L. Lu, M. C. Rechtsman, D. Schuster, J. Simon, O. Zeitler, and I. Carusotto, "Topological photonics," *Rev. Mod. Phys.* **91**, 015006 (2019).
 30. W. Hu, J. C. Pillay, K. Wu, M. Pasek, P. P. Shum, and Y. D. Chong, "Measurement of a topological edge invariant in a microwave network," *Phys. Rev. X* **5**, 011012 (2015).
 31. A. D'Errico, F. Cardano, M. Maffei, A. Dauphin, R. Barboza, C. Esposito, B. Piccirillo, M. Lewenstein, P. Massignan, and L. Marrucci, "Two-dimensional topological quantum walks in the momentum space of structured light," *Optica* **7**, 108–114 (2018).
 32. S. Mittal, S. Ganeshan, J. Fan, A. Vaezi, and M. Hafezi, "Measurement of topological invariants in a 2D photonic system," *Nat. Photonics* **10**, 180–183 (2016).
 33. Y. Bromberg, Y. Lahini, and Y. Silberberg, "Bloch oscillations of path-entangled photons," *Phys. Rev. Lett.* **105**, 263604 (2010).
 34. G. Corrielli, A. Crespi, G. Della Valle, S. Longhi, and R. Osellame, "Fractional Bloch oscillations in photonic lattices," *Nat. Commun.* **4**, 1555 (2013).
 35. D. Witthaut, F. Keck, H. J. Korsch, and S. Mossmann, "Bloch oscillations in two-dimensional lattices," *New J. Phys.* **6**, 41 (2004).
 36. F. Bloch, "Über die Quantenmechanik der Elektronen in Kristallgittern," *Z. Phys.* **52**, 555–600 (1929).
 37. E. Haller, R. Hart, M. J. Mark, J. G. Danzl, L. Reichsöllner, and H.-C. Nägerl, "Inducing transport in a dissipation-free lattice with super Bloch oscillations," *Phys. Rev. Lett.* **104**, 200403 (2010).
 38. M. Ben Dahan, E. Peik, J. Reichel, Y. Castin, and C. Salomon, "Bloch oscillations of atoms in an optical potential," *Phys. Rev. Lett.* **76**, 4508–4511 (1996).
 39. T. Pertsch, P. Dannberg, W. Elflein, A. Bräuer, and F. Lederer, "Optical Bloch oscillations in temperature tuned waveguide arrays," *Phys. Rev. Lett.* **83**, 4752–4755 (1999).
 40. R. Morandotti, U. Peschel, J. S. Aitchison, H. S. Eisenberg, and Y. Silberberg, "Experimental observation of linear and nonlinear optical Bloch oscillations," *Phys. Rev. Lett.* **83**, 4756–4759 (1999).
 41. G. Lenz, I. Talanina, and C. M. de Sterke, "Bloch Oscillations in an array of curved optical waveguides," *Phys. Rev. Lett.* **83**, 963–966 (1999).
 42. H. Trompeter, W. Krolikowski, D. N. Neshev, A. S. Desyatnikov, A. A. Sukhorukov, Y. S. Kivshar, T. Pertsch, U. Peschel, and F. Lederer, "Bloch oscillations and Zener tunneling in two-dimensional photonic lattices," *Phys. Rev. Lett.* **96**, 053903 (2006).
 43. S. Longhi, "Optical Zener-Bloch oscillations in binary waveguide arrays," *Europhys. Lett.* **76**, 416–421 (2006).
 44. F. Dreisow, A. Szameit, M. Heinrich, T. Pertsch, S. Nolte, A. Tünnermann, and S. Longhi, "Bloch-Zener oscillations in binary superlattices," *Phys. Rev. Lett.* **102**, 076802 (2009).
 45. M. Levy and P. Kumar, "Nonreciprocal Bloch oscillations in magneto-optic waveguide arrays," *Opt. Lett.* **35**, 3147–3149 (2010).
 46. P. Xue, R. Zhang, H. Qin, X. Zhan, Z. H. Bian, J. Li, and B. C. Sanders, "Experimental quantum-walk revival with a time-dependent coin," *Phys. Rev. Lett.* **114**, 140502 (2015).
 47. C. Cedzich and R. F. Werner, "Revivals in quantum walks with a quasiperiodically-time-dependent coin," *Phys. Rev. A* **93**, 032329 (2016).
 48. U. Peschel, C. Bersch, and G. Onishchukov, "Discreteness in time," *Open Phys.* **6**, 619–627 (2008).
 49. C. Bersch, G. Onishchukov, and U. Peschel, "Experimental observation of spectral Bloch oscillations," *Opt. Lett.* **34**, 2372–2374 (2009).
 50. L. Yuan and S. Fan, "Bloch oscillation and unidirectional translation of frequency in a dynamically modulated ring resonator," *Optica* **3**, 1014–1018 (2016).
 51. C. Cedzich, T. Rybár, A. H. Werner, A. Alberti, M. Genske, and R. F. Werner, "Propagation of quantum walks in electric fields," *Phys. Rev. Lett.* **111**, 160601 (2013).
 52. M. Genske, W. Alt, A. Steffen, A. H. Werner, R. F. Werner, D. Meschede, and A. Alberti, "Electric quantum walks with individual atoms," *Phys. Rev. Lett.* **110**, 190601 (2013).
 53. L. A. Bru, M. Hinarejos, F. Silva, G. J. de Valcárcel, and E. Roldán, "Electric quantum walks in two dimensions," *Phys. Rev. A* **93**, 032333 (2016).
 54. C. Cedzich, T. Geib, A. H. Werner, and R. F. Werner, "Quantum walks in external gauge fields," *J. Math. Phys.* **60**, 012107 (2019).
 55. H. Chalabi, S. Barik, S. Mittal, T. E. Murphy, M. Hafezi, and E. Waks, "Synthetic gauge field for two-dimensional time-multiplexed quantum random walks," *Phys. Rev. Lett.* **123**, 150503 (2019).
 56. D. H. Dunlap and V. M. Kenkre, "Dynamic localization of a charged particle moving under the influence of an electric field," *Phys. Rev.* **B34**, 3625–3633 (1986).
 57. G. Lenz, R. Parker, M. Wanke, and C. de Sterke, "Dynamical localization and AC Bloch oscillations in periodic optical waveguide arrays," *Opt. Commun.* **218**, 87–92 (2003).
 58. S. Longhi, M. Marangoni, M. Lobino, R. Ramponi, P. Laporta, E. Cianci, and V. Foglietti, "Observation of dynamic localization in periodically curved waveguide arrays," *Phys. Rev. Lett.* **96**, 243901 (2006).
 59. R. Iyer, J. S. Aitchison, J. Wan, M. M. Dignam, and C. M. de Sterke, "Exact dynamic localization in curved AlGaAs optical waveguide arrays," *Opt. Express* **15**, 3212–3223 (2007).
 60. A. Joushaghani, R. Iyer, J. K. S. Poon, J. S. Aitchison, C. M. de Sterke, J. Wan, and M. M. Dignam, "Quasi-Bloch oscillations in curved coupled optical waveguides," *Phys. Rev. Lett.* **103**, 143903 (2009).
 61. A. Joushaghani, R. Iyer, J. K. S. Poon, J. S. Aitchison, C. M. de Sterke, J. Wan, and M. M. Dignam, "Generalized exact dynamic localization in curved coupled optical waveguide arrays," *Phys. Rev. Lett.* **109**, 103901 (2012).
 62. L. Yuan and S. Fan, "Three-dimensional dynamic localization of light from a time-dependent effective gauge field for photons," *Phys. Rev. Lett.* **114**, 243901 (2015).
 63. V. V. Orre, E. A. Goldschmidt, A. Deshpande, A. V. Gorshkov, V. Tamma, M. Hafezi, and S. Mittal, "Interference of temporally distinguishable photons using frequency-resolved detection," *Phys. Rev. Lett.* **123**, 123603 (2019).
 64. H. Pichler, S. Choi, P. Zoller, and M. D. Lukin, "Universal photonic quantum computation via time-delayed feedback," *Proc. Natl. Acad. Sci. USA* **114**, 11362–11367 (2017).
 65. H. Chalabi and E. Waks, "Interaction of photons with a coupled atom-cavity system through a bidirectional time-delayed feedback," *Phys. Rev. A* **98**, 063832 (2018).